Near-shore wave power characterized with a remotely controlled surface vehicle in Admiralty Inlet, Puget Sound, WA

Trevor Uptain[1]

[1]University of Washington, School of Oceanography, Box 35790, Seattle, WA, 98195-5060
Advisor: Miles Logsdon
(505) 543-5060
trevoru@uw.edu

Abstract

Wave power availability in Admiralty Inlet, Puget Sound, WA (USA) was assessed using measurements from a surface wave characterization vehicle. The device was designed to analyze wind and wave power, with each instrument evaluated modularly prior to the experiment to control for error. Data was collected across several transects within the strait and analyzed to determine the cross-sectional wave power of the system. The spatial variability of the energy resource was characterized using data collected from the instrument, while temporal availability was resolved using mean field models. The method was demonstrated to be an effective predictor of localized temporal predictability based on immediate wind conditions, with significant limitations on its use for site selection without continuous monitoring.

1. Introduction

Admiralty Inlet is a narrow strait forming the marine entrance to Puget Sound in Washington State, USA. The Inlet was formed during the last glacial retreat, which created a shallow underwater sill between present-day Whidbey Island and the Olympic peninsula. Given the tidal forces present in the sill, it has been previously considered as a site for underwater power conversion. Recent attempts have been made to characterize the wave energy resource in this locality (Polagye & Thomson, 2013), as well as in nearby locations in the Pacific Northwest (Lenee-Bluhm, 2011). These efforts are a small subset of studies conducted worldwide attempting to

characterize local variations in wave power. As underwater power conversion technology has progressed, the goal of utilizing wave energy to produce electrical energy has become increasingly plausible — even on a large scale.

This study investigates the temporal and spatial effects of wind fetch on surface waves in a near-shore system in Puget Sound, with fetch defined as the length of water over which a given wind has blown. The goal is to describe the relationship between fetch and variation in gross wave power throughout the water column, and to construct a model of local availability of wave power based on variations in wind conditions. Previous work has attempted to assess the wave energy resource along kilometer-scale stretches of Vancouver Island (Cornetti, 2014), along with several other coastal areas of interest from around the world. However, this effort is novel in its collection of high-resolution spatial data, which can potentially be used to correct previous methods used to estimate wave energy. This is important since the ability to rapidly assess the wave power of a near-shore system has important implications for several areas of coastal engineering interest. The vulnerability of coastal environments to catastrophic events, such as an oil spill, are dependent not only on circulation but on physical processes which control the flux of water in the system (Gundlach, 1978). With a knowledge of the wave power present in a local system, structurally vulnerable coastlines could be assessed with increased speed and accuracy since the rate of coastal erosion is dependent on the assailing force of the waves (Sunamura, 1977).

Lastly, while the technology to harness wave energy exists, the first barrier to widespread development of wave farms is the difficulty in identifying locations to install them (Reikard, 2015). A sensor built to characterize local wave energy might be used to quickly identify potential sites for energy production — or to exclude them from candidacy.

No attempt has been made to analyze the energy of a near shore system with the use of a continuously-run surface vehicle. The use of such an instrument could provide high-resolution data to modify scientific understanding of near-shore wave energy. Previous studies have typically utilized buoys to make measurements of wave height, which provides excellent temporal resolution. However, since the number of buoys is limited, spatial coverage is patchy at best. Using a vehicle which can make measurements along transects, an experiment was conducted to determine the surface wave energy of a particular region in Puget Sound. The results were analyzed to test the effect of wind direction on wave power variation, and extrapolated to the water column mathematically. The sensors were tested in the field and analyzed for accuracy to determine the comprehensiveness of the data collected.

The results from this experiment were used to analyze the effect of wind conditions on wave power availability in Admiralty Inlet.

2. Methods

A surface wave characterization vehicle, equipped with a GPS unit and an accelerometer, was deployed from a shore station to run 50 meter, straight line transects at various angles from the point of origin. The site chosen for the study was at the southernmost point of Admiralty Head, with the first transect running southward. Throughout deployment, wind speed and direction were recorded, along with the angle of wave propagation relative to shore. The first transect ran parallel to wind direction, with the second deployment at a right angle. A third deployment ran directly perpendicular to shore, while the angle of the fourth and fifth were chosen to maximize coverage (Figure 1).

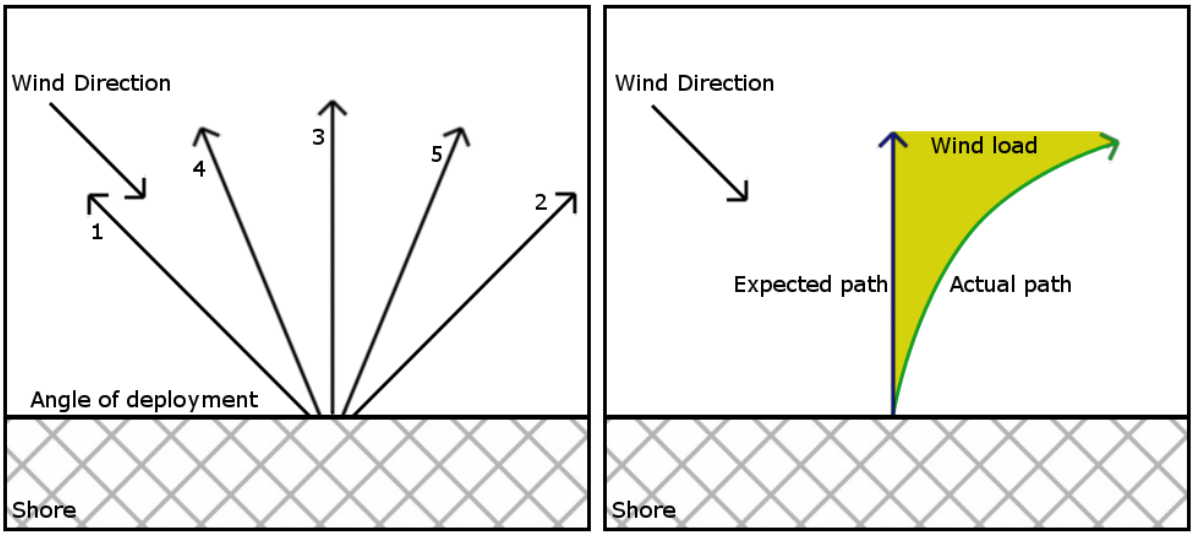

Figure 1 — The graphic on the left is illustrative of the angles of deployment chosen to analyze wind characteristics. The first transect runs against the wind, while the second runs at a complementary angle. The third runs perpendicular to the shore, and the final transects maximize coverage. The graphic on the right shows how wind load was measured over the course of a single run. The deviation of the vehicle from the expected path is a function of wind velocity, as well as surface area and mass of the vehicle. This allows for a determination of the effect of wind on surface waves.

Upon completion of the transect, the system was automatically shut down and pulled back to shore with a tether attached to the vehicle.

Over the course of the run, the vehicle drifted from its expected path due to wind load. Deviation from the expected path is a function of wind velocity surface area of the vehicle, mass of the vehicle, and a drag coefficient, which was used to make deterministic calculations for wind load (Figure 1). The results were then compared to wind velocity recorded from shore during the run.

Using GPS data, the instantaneous velocity of the system was determined along the course of each transect. Bathymetry data was acquired from a U.S. Geological Survey of the area, with measured accuracy within 20cm. Combining these with data from the accelerometer, the variable magnitude and frequency of z-axis surface waves along the transect were calculated. Angular frequency of the waves were then determined and used to find the wavenumber k (Lenee-Bluhm, 2011):

$$(2\pi f)^2 = gk \tanh kh$$

Where f is frequency, g is acceleration due to gravity, and h is the depth of the water column. This allowed for the determination of group velocity:

$$c_g = \frac{\pi f}{k}\left(1 + \frac{2kh}{\sinh 2kh}\right)$$

The energy flux transmitted by a regular wave per unit crest width can be written as a vertical section of unit width, perpendicular to the wave propagation direction (Contestabile, 2015). The power (in $kg*m*s^{-3}$) is therefore given by:

$$P = 1/8\ \rho\ g\ h^2\ C_g$$

Where C_g represents group velocity and ρ is water density. Now, power has been calculated in a form wherein it can be compared to any other given site.

Based on accuracy in field tests, an equation derived in a study by Hasselman et al. was used to determine fetch:

$$F = [(1.85g^{0.77}\ (U \cos \theta)^{-0.54}) / f_p]^{-4.35}$$

Where F is fetch, U is wind speed, θ is the angle of the wave from mean wind direction, and f_p is peak frequency.

3. Results

Instrument Performance

The deployment of the system was a successful component of this study, producing synchronous data throughout each transect. Despite heavy wind and wave conditions, both of the vehicle's thrusters remained submerged for the duration of the trial. The experiment raised questions about the accuracy of the sensors given the

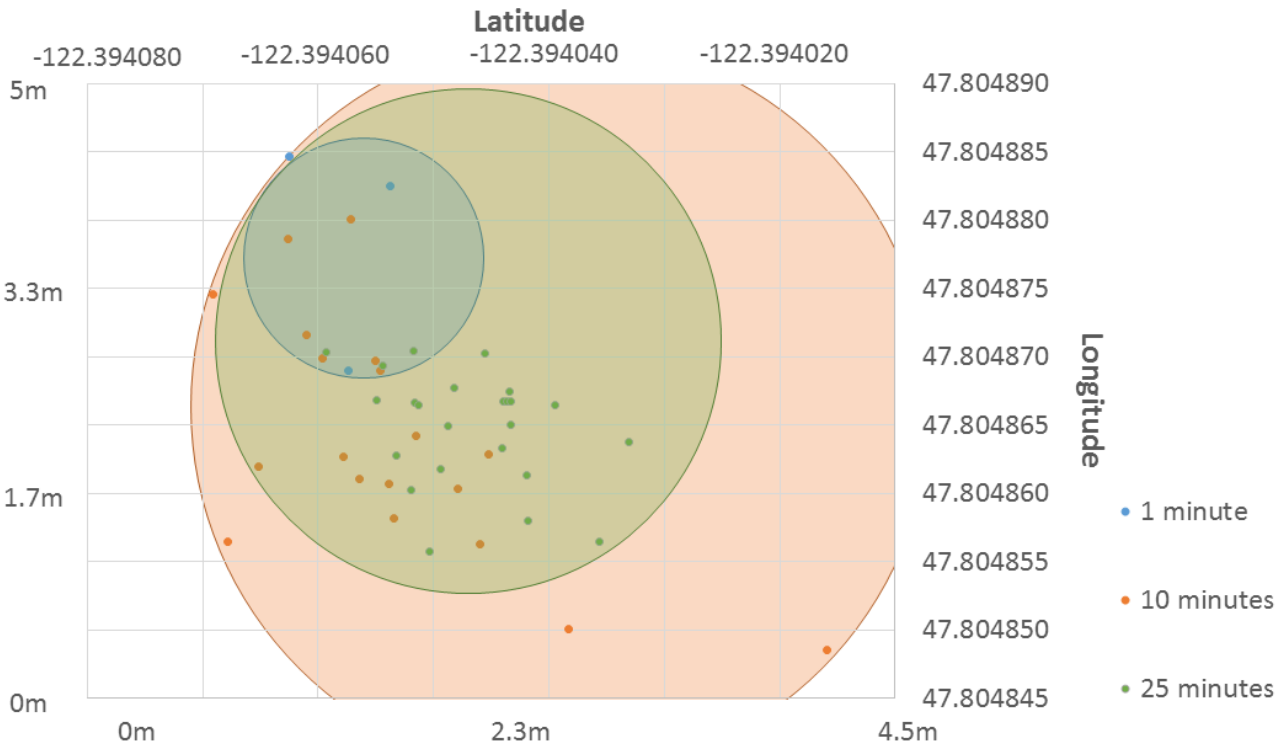

Figure 2 — This graphic shows the data recorded from a stationary GPS unit over a 25 minute interval. Increasing error in recorded location is demonstrated over recording times of 1 minute, 10 minutes, and 25 minutes. The diameter of a given circle is a determination of the potential error in position location over that time period.

strong wind and wave gradients along the transect. The duration of data collection, which has the potential to cause 'drift' in some instruments, was of equal concern. This uncertainty was controlled by experimentation prior to work in the field. The GPS was left to collect data in a spot near the sample site for 25 minutes, demonstrating drift and a potential error of up to 6 meters in determining location (Figure 2). The high sampling rate of the accelerometer produced significant noise, and was therefore treated using a simplified Kalman filter (Singhal, 2012) and tested for accuracy at several known frequencies and magnitudes. A second filter was used to determine

peak frequency. Figure 3 suggests that error in accelerometer data increases as acceleration increases, while the filter becomes less capable of identifying peak acceleration at higher magnitudes. Finally, the wind speed sensor was calibrated against a commercial standard and produced a maximum error of ± 0.3 km/h, with standard error uniform across a range of expected velocities. This sensor begins to show increased error at wind speeds of ~5 km/h, and is incapable of producing a reading at speeds greater than 14 km/h. However, at no point during the experiment were such extreme conditions present.

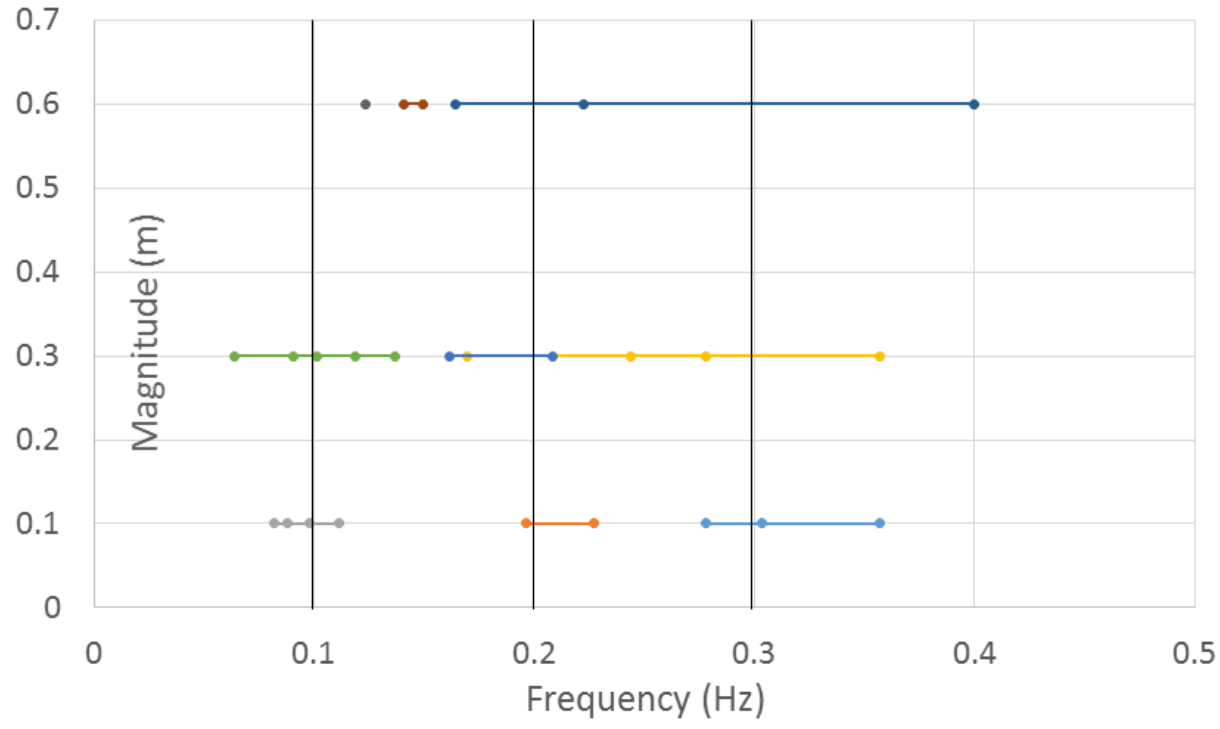

Figure3 — Error in measured frequency increases as the magnitude of the wave increases. The colored lines represent the measured values, while the dark, vertical lines represent the expected frequency.

Experimental Results

The experiment yielded non-trivial statistical differences in velocity between runs using a one-tail significance test, justifying an estimate of surface wave power parameterized by wind direction and the above-water surface area of the vehicle exposed to wind force. Figure 4 demonstrates the differences in average velocity between each run which, as expected, decrease as the angle of the transect departs from transects opposed to wind direction.

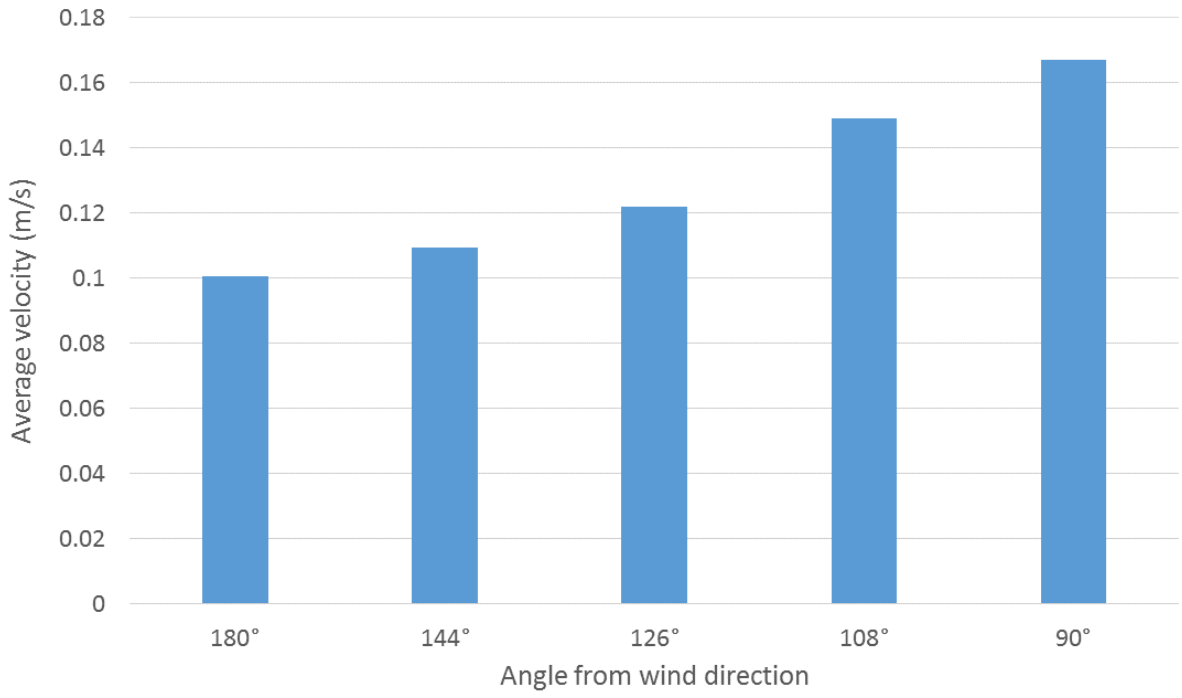

Figure 4 — The instrument was deployed at several angles relative to wind direction. This graph demonstrates the increase in average velocity of the run as the starting angle is increasingly removed from deployment directly into the wind. Each velocity is averaged over eight runs.

Instantaneous velocity is demonstrably larger over the course of those runs which propagate away from the angle of wind direction (Figure 5). Notably, instantaneous velocity tends to increase at the beginning of the transect near the shore where shallow bathymetry increases wave velocity. It peaks as the wave height increases, then begins to decline again as the instrument is exposed to winds and surface waves.

The experiment yielded an estimate for the force of wind on the vehicle, or wind load. This was based on the deviation from the vehicle's expected trajectory, accounting for the surface area of the vehicle and a drag coefficient for the submerged

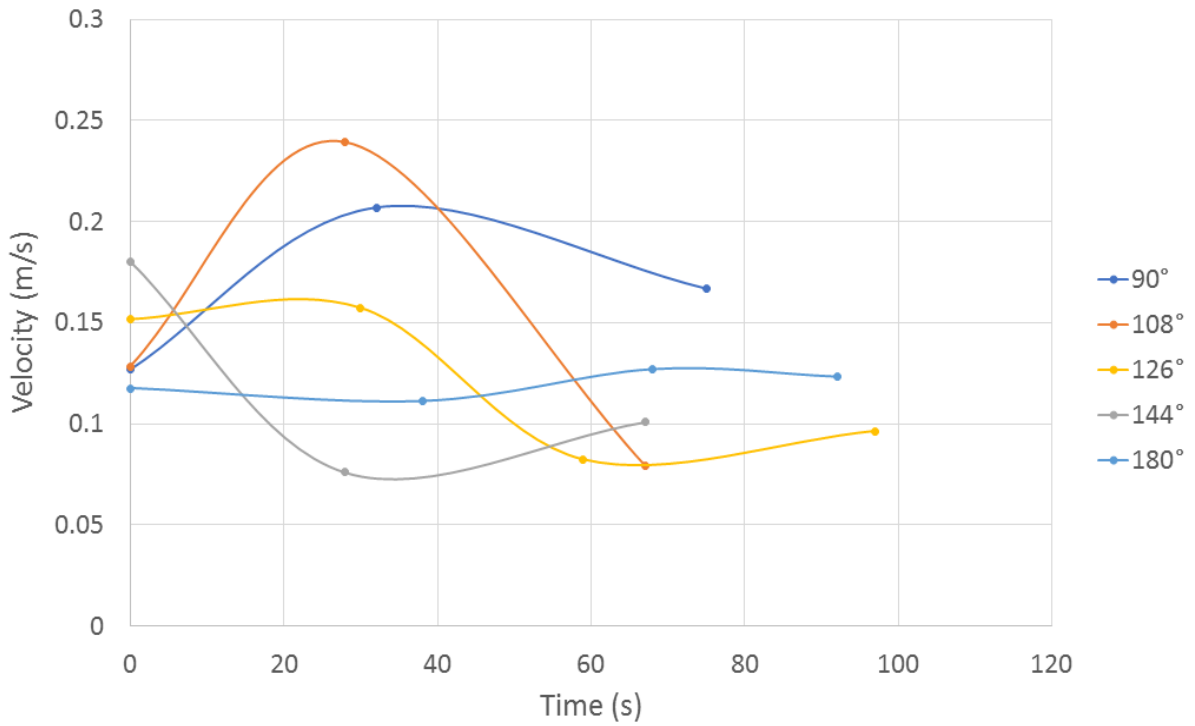

Figure 5 — This plot shows how the velocity varies over each run dependent on the angle of deployment. Velocity was calculated from time and location data recorded by the GPS unit. This graph represents a single set of runs with wind direction opposing 108°.

portion of the vehicle. Wind velocity was calculated from this determination, with a maximum variation from measured wind speed of 0.65 m/s. Wave power (in kW/m^2) was determined using measured wind speed data and estimates of wave frequency, wavelength, wavenumber, and group velocity based on analysis of collected data. Wave power estimates varied little over the course of the eight runs, which was anticipated given fairly constant wind conditions over the course of the experiment. Finally, fetch was determined using the equation from Hasselman et al.

Run	Wind load, kg	Wind velocity (calculated), m/s	Wind velocity (measured), m/s	Wave power, kW/m^2	Fetch, km
1	0.42	6.04	6.05	2.30	11.40
2	0.50	6.56	6.43	2.44	11.11
3	0.46	6.32	6.62	2.51	10.82
4	0.43	6.07	6.49	2.46	11.06
5	0.48	6.45	6.25	2.37	11.41
6	0.41	5.92	6.16	2.33	11.78
7	0.53	6.74	6.09	2.31	11.44
8	0.39	5.82	6.21	2.36	11.20
$\bar{x}$	0.45	6.24	6.29	2.38	11.27
σ	0.05	0.33	0.20	0.08	0.29

Table 1 — Calculations for wind load, calculated and measured wave velocity, wave power, and fetch are shown averaged across each run. Wind load was calculated from the deviation of the instrument from its expected path and used to determine calculated wind velocity. Measured velocity came from an onshore instrument. Wave power was determined using parameters determined by velocity, accelerometer, and GPS data collected by the system. These measurements were further derived to determine fetch.

4. Discussion

Table 1 demonstrates a low standard deviation for each variable derived from the experiment. Instrument error outlined in the previous section is significant, and although the results are precise, their accuracy may be called into question based on consistent error introduced during measurements from the GPS and accelerometer.

The average velocity does not say much about energy availability of the system. However, it is useful as a reference point for determining the causes of change in instantaneous velocity, which is not only necessary for calculations of systemic wave power, but is also important in discerning the affect that wind has on surface waves. Plotted against time, variations in velocity are significant throughout the course of each run. Accordingly, the average results presented in Table 1 are not indicative of the significant variability which occurred during the course of the experiment. Further, measurements taken in shallow water are not very useful in determining wave power without data transformations applied for shoaling and breaking waves. To account for this, the results in Table 1 reflect only the latter half of each run where the depth is >15m.

The most significant information derived from the study is the calculation of cross-sectional wave power determined by the surface vehicle. In a study conducted in Admiralty Inlet in 2013, Polagye determined a range of values for wave power

availability based on a year-long study conducted with Acoustic Doppler Current Profiler (ADCP) data. The results of that study in the area nearest the experiment conducted in this one conclude that there is an average cross-sectional power availability of ~1.8 kW/m^2. Comparing this to our result of an average of 2.38 kW/m^2, we see that the power availability determined by this study is significantly higher according to a two-tail significance test. Although this could be accounted for by rough wind conditions on the day of the study, the wind velocity during the experiment was not much higher than average. Since the study was conducted over a relatively short period of time, it is possible that there was some other variable which affected the temporal wave power on that particular day. However, it is more likely that there is systematic error introduced into the calculations by accelerometer error, that the drag coefficient used in the calculations used incorrect parameters, or especially that a poor accounting for tidal forces affected the results of the experiment. Without repeated experimentation over a long period of time, it would be difficult to determine exactly what caused the error.

The estimates for fetch distance are unreasonably high based on local topographical features, which is unsurprising given that the parameters used to calculate wave power were also used to determine fetch. However, given the relative agreement between measured and calculated wave fetch, it appears as if the calculations for wind load were accurate. This implies that the GPS data collected by

the instrument was accurate, and strengthens the case for instrument error introduced by the accelerometer. Given the calculations made to assess the validity of the accelerometer data, it seems reasonable to assume that this one sensor was the single largest barrier in making accurate determinations of wave power in this region.

5. Conclusions

The accuracy of the system in predicting wind speed suggests that the methods used in this study are useful for characterizing local wave power conditions at specific locations at specific times. The high resolution spatial data provided by the instrument could be beneficial for improving the understanding of power gradients during studies measuring power availability with other instruments, such as ADCPs or buoys. Without further experimentation, reduction in instrument error, and data collected over significant lengths of time in areas where comparison is possible, it is difficult to determine whether the instrument used in this study is capable of predicting wave resource availability in a manner which is useful to coastal ecologists and power conversion companies. Results indicate the need for more precise accelerometer data in order to make accurate assessments of wave power. Reconciliation of the data to tidal models would also improve the accuracy of future predictions.

6. References

Bryson R.D. Robertson, C. E. (2014). Characterizing the near shore wave energy resource on the west coast of Vancouver Island, Canada. *Renewable Energy, 71*, 665-678.

Contestabile, P. F. (2015). Wave Energy Resource along the Coast of Santa Catarina (Brazil). *Energies, 8*, 14219-14243.

Cornetti, A. T. (2014). Appraisal of IEC Standards for Wave and Tidal Energy Resource Assessment. *International Conference on Ocean Energy, Halifax, Canada*, 1-11.

D.G. Mediavilla, H. S. (2016). Nearshore assessment of wave energy resources in central Chile. *Renewable Energy, 90*, 136-144.

Epler, J., Polagye, B., & Thomson, J. (2010). Shipboard Acoustic Doppler Current Profiler Surveys to Assess Tidal Current Resources . *OCEANS 2010 MTS/IEEE SEATTLE* , 1-10.

Gundlach, E. R. (1978). Vulnerability of coastal environments to oil spill impacts. *Marine Technology Society Journal, 12*(4), 18-27.

Hasselmann, K. B. (1973). Measurements of wind-wave growth and swell decay during the Joint North Sea Wave Project (JONSWAP). *Herausgegeben vom Deutschen Hydrographischen Institut, 8*(12).

Lenee-Bluhm, P. P.-H. (2011). Characterizing the wave energy resource of the US Pacific Northwest. *Renewable Energy, 36*.

Munk, W. (1955). Wind stress on water: an hypothesis. *Quarterly Journal of the Royal Meteorological Society, 81*(349), 320-332.

Polagye, B., & Thomson, J. (2013). Tidal energy resource characterization: methodology and field study in Admiralty Inlet, Puget Sound, US. *Proceedings of the Institution of Mechanical Engineers, Part A: Journal of Power and Energy*.

Reikard, G. R.-R. (2015). Simulating and forecasting ocean wave energy in western Canada. *Ocean Engineering, 103*, 223-236.

Singhal, T. H. (2012). Kalman Filter Implementation on an Accelerometer sensor data for three state estimation of a dynamic system. *International Journal of of Research in Engineering and Technology*, 2277-4378.

Sunamura, T. (1977). A Relationship Between Wave-induced Cliff Erosion and Erosive Force of Waves. *The Journal of Geology, 85*(5), 613-618.

Appendix A — Design Rationale

Design Summary

The system is comprised of a watertight pressure housing attached to a positively buoyant float. Two mechanical arms extend from the pressure housing, each hosting a submersible thruster motor. A 12V battery inside the pressure housing provides power for the entire system, which includes the motors, GPS, accelerometer, and a microcontroller.

Mechanical Structure

The vehicle's pressure housing utilizes a waterproof Pelican™ Case. The housing has a hole drilled in either side, overlaid on the outside with a sleeve to mount the PVC arms. The arms provide structural support for the thrusters, as well as providing a conduit for routing the thruster cables into the pressure housing. The arms extend 1.5 meters below the housing to prevent the thrusters from swinging out of the water, even when the vehicle is propagating through high intensity waves. The end of the arms are fitted with a watertight pass-through to prevent water from leaking into the housing, although the conduits into the housing are filled with foam as a precautionary

measure. The entire system rests on a ring of floats bound together with pipe clamps, and is attached to it with lashing winch tie-downs. Two pass-throughs are installed at the top of the pressure housing to 1) allow the GPS antenna to extend outside the case and 2) provide structural support for a flag to increase visibility. As a unit, the system is highly positively buoyant.

Sensors

The vehicle is equipped with two sensors. The first is an off-the-shelf GPS unit which can be tracked from a shore module. In order to confirm the accuracy of the tracking system, data will be logged from the stationary GPS unit at increasing time intervals and analyzed for error. This will be done at the site of the experiment to increase the relevance of the results.

The second sensor is an accelerometer, which will be used to measure multidirectional variation in acceleration as the vehicle runs along its transect.

Power supplied to the Arduino from the battery is stepped down to 5V with a DC-DC converter.

Electronics and Software

The Arduino microcontroller is a highly interactive device which allows for the operation of multiple electronic devices from a single board. It controls both the

thruster motors and a triple axis accelerometer. For this experiment, the thrusters will be programmed to rotate at low RPM for a set time interval. This allows for simpler recovery of the vehicle after it completes a transect. The intermediary between a thruster and the Arduino is an Electronic Speed Controller (ESC) provided by the manufacturer of the thruster. This reduces the task of programming the microcontroller to a reasonable level of simplicity.

Input from the accelerometer is processed by the Arduino and stored on a microSD card. This is accomplished through the use of a datalogger shield, which is designed to be compatible with the Arduino. The rate of collection is carefully controlled in order to obtain complete data while still reserving enough memory to complete the transect.

The code which controls the system is modified from several online repositories.

Appendix B — Systems Flowchart